

# Face Attributes as Cues for Deep Face Recognition Understanding

Matheus Alves Diniz and William Robson Schwartz

Smart Sense Laboratory,  
Department of Computer Science,  
Federal University of Minas Gerais, Brazil  
{matheusad,william}@dcc.ufmg.br

**Abstract**—Deeply learned representations are the state-of-the-art descriptors for face recognition methods. These representations encode latent features that are difficult to explain, compromising the confidence and interpretability of their predictions. Most attempts to explain deep features are visualization techniques that are often open to interpretation. Instead of relying only on visualizations, we use the outputs of hidden layers to predict face attributes. The obtained performance is an indicator of how well the attribute is implicitly learned in that layer of the network. Using a variable selection technique, we also analyze how these semantic concepts are distributed inside each layer, establishing the precise location of relevant neurons for each attribute. According to our experiments, gender, eyeglasses and hat usage can be predicted with over 96% accuracy even when only a single neural output is used to predict each attribute. These performances are less than 3 percentage points lower than the ones achieved by deep supervised face attribute networks. In summary, our experiments show that, inside DCNNs optimized for face identification, there exists latent neurons encoding face attributes almost as accurately as DCNNs optimized for these attributes.

## I. INTRODUCTION

Deeply learned face representations are currently employed in many state-of-the-art methods for face recognition [3, 33]. These representations are obtained from Deep Convolutional Neural Networks (DCNNs) which are optimized to discriminate thousands of individuals. The superiority of DCNN features is related to their depth [15]. Between the input image and the final classification layer there are dozens of hidden layers. Each such layer learns a latent representation of the original image based on the output of the previous layer. The final hidden layer is connected to an output layer which is usually supervised under the tasks of identification, verification or both [23].

The meaning of each neuron in the output layer is defined by the user, and thus can be precisely explained. For instance, in the identification task, each neuron represents an identity, and therefore should only be activated for inputs from the same individual. However, the activation patterns of the output layer are specific to the training set. Thus it is preferred to use features from one of the hidden layers as the representation for a generic face image. While this choice is effective, neurons from these layers are latent features that are not easy to interpret. Therefore, it becomes challenging to explain the behavior of such recognition systems. Besides the improvement of user confidence, understanding the nature of



Fig. 1. Average faces of the top-100 and bottom-100 activations of six selected neurons of a ResNet50 deep network that was optimized for face identification. Each neuron is identified by the attribute that it discriminates and its layer depth.

DCNNs features could also lead to new insights on how to increase the performance of these networks.

Recently, several efforts have been dedicated to explaining the behavior of DCNNs. Visualization techniques are, perhaps, the most popular methods amidst such efforts. Instead of analyzing the raw output of a neuron, these methods create or modify images to portray the patterns observed by that neuron. For instance, some methods maximize the output of neuron with respect to the input image [27]. When this neuron corresponds to some object class, the optimized input image will contain patterns that resemble the object category. By visualizing these images, users can diagnose the networks to both understand failure cases as well as to gain intuition regarding the learning process.

One inherent limitation of visualization techniques is their qualitative nature. This aspect may limit their applicability since their results are often open to subjective interpretation. Another limitation of visualization approaches is scalability. Fine-grained analysis of individual feature-maps or neurons of the DCNNs is especially difficult to achieve. A deep network may contain thousands of filters across its hidden layers, and even more neurons. Generating one image for each unit would be impractical due to time constraints and the amount of generated images to be manually analyzed.

Discovering the meaning of each neuron in a network is an onerous task. Besides the excessive number of neurons in a network, some of them may also encode latent features that have no precise meaning for humans [34]. To circumvent these adversities, we invert our goal. Instead of observing a neuron to discover its meaning, we establish a few concepts that are likely to be represented in the network and try to determine which neurons encode them. Particularly, we investi-

gate the concepts learned by a deep face recognition network. Our hypothesis is that face attributes are encoded inside the DCNN, since some of these attributes are relevant for recognition. To verify this assumption, we train a traditional machine learning pipeline to predict face attributes from the output of the hidden layers. The accuracy of the predictor is used as an indicator of how well each attribute is implicitly learned by the network. To handle the high-dimensionality of the hidden layers, we employ Partial Least Squares (PLS) [1] to create a discriminative low-dimensional projection for each attribute. We then identify the most relevant neurons in the low-dimensional space using the Variable Importance in Projection (VIP) technique. Fig. 1 shows a visualization of six neurons that were identified with our approach. For each neuron we show pair of images representing an average face of the inputs that presented the highest and lowest activations.

According to our experimental results, a single neuron in the recognition network can achieve, for some attributes, an accuracy exceeding 96%, which is less than 3 percentage points (p.p.) lower than a fully supervised face attribute DCNN. Such extraordinary performance demonstrates that face recognition DCNNs are able to implicitly learn these semantic concepts without any supervision. To the best of our knowledge, this is the first work that was able to provide a thorough analysis of DCNNs using latent features as input for classifiers.

## II. RELATED WORKS

The performance of automatic face recognition soared in the last years. Deeply learned features coupled with immense amounts of data [2, 13] are the main source of this improvement. State-of-the-art convolutional neural networks are trained to classify thousands of identities, resulting in latent representations inside the network that are very robust and discriminative [3, 4, 28]. Deep networks can also be used to learn face attributes such as gender, age or hair color [16]. Besides the direct application in retrieval, these attributes are also beneficial to other methods such as verification, identification and localization [21]. In this work, we are not concerned with outperforming benchmarks on any of these tasks. Instead, we want to understand the learning of process of deep face recognition networks, specifically of face attributes encoding inside the network.

Many attempts to understand DCNNs consist of visualizing the learned filters of intermediate layers. Some approaches attach a deconvolutional [32, 34] or up-convolutional [5] network to a layer of the DCNN to revert its feature maps back to the pixel space. Other approaches rely on backpropagation to visualize images that are good representations of some features of the network [17, 19, 27, 31]. This is achieved by optimizing a neural activation pattern with respect to the input image, adjusting the input to match or maximize the desired pattern. However, regardless of the method, it is unfeasible to visualize all filters inside a network, specially with the growing size of network architectures. Furthermore, the conclusions obtained by these

approaches may be biased since assigning semantic meaning to the obtained images is a subjective task. Human operators are able to find interpretable meaning for network patterns even when they are changed to a random basis [30].

The aforementioned limitations can be mitigated through a more quantitative methodology. Some methods are able to visualize the region in the input image that is more relevant for the classification output [25, 35, 36]. In an image classification context, these regions represent the localization of the class object in the image. When compared to other methods that are supervised for localization, these methods still have a mildly competitive performance, demonstrating that DCNNs supervised only for classification encode information relevant for object detection.

Deep face recognition contains few particularities that distinguishes it from other DCNNs. Traditionally, the supervised output of the training phase is also the desired output of testing phase. Face recognition networks, on the other hand, act as a feature extractor at this second phase. The supervised layer is removed, and the features of a hidden layer are used along with another learning method or distance metric. Thus, the output layer analysis is not as useful for face recognition networks.

The attempts to understand face recognition networks are concentrated on the analysis of the hidden neurons. Examination of neuron activations revealed that even a single neuron is highly discriminative for some face attributes or even specific identities [6, 16, 29]. Furthermore, the neural activation pattern also encodes the quality of the input image. A feature with low L2-norm strongly indicates a hard to recognize input face in a DCNN supervised for face identification [20]. Visualization techniques have limited usage in hidden layer analysis because latent features do not necessarily encode any interpretable meaning for humans. However, a few interpretable feature maps can be found by detecting high activation patterns for visually similar images [34].

Our approach engages the face recognition problem in a different manner. Instead of visualizing or measuring activation patterns in the network to define their meaning, we start from a set of attributes that are likely to be encoded in the network and then use traditional machine learning techniques to determine which features encode them. Specifically, we train and validate an attribute classifier with the outputs of each layer in the network, and use its weights and performance to infer how the recognition behaves. The usage of classifiers using middle-level representations of the network has been previously studied in other contexts such as transfer learning [32], hypernets [11, 14], early predictions [26] and network pruning [12].

## III. PROPOSED APPROACH

We present a method to analyze deep face recognition networks. For each layer of the network, we attach and train a face attribute classifier and use its accuracy as an indicator of how well a face attribute is encoded in that layer. We believe that using the classifier performance as our indicator,

diminishes the effect of the human bias that is present in some visualization techniques.

One challenging aspect of our methodology is the high dimensionality of the latent feature maps, which can exceed 800,000 dimensions. For such high-dimensional spaces, classical learning algorithms are impractical to train due to small sample size, slow convergence or expensive computation. There is also a concern not to interfere too much with the network representation. For instance, using a convolutional sub-network as our classifier could add semantic information that was not present in the original feature map.

In this context, dimensionality reduction techniques are suitable candidates to overcome these problems. Specifically, PLS [1] was previously shown to be capable of dealing with dimensionalities as high as 170,000 [24]. In its essence, PLS decomposes the flattened network features,  $X$ , and the attributes matrix,  $Y$  into

$$X = TP^T + E \quad (1)$$

$$Y = UQ^T + F \quad (2)$$

where  $T$  and  $U$  are the extracted low-dimensional factors,  $Q$  and  $P$  contain the loadings, and  $E$  and  $F$  represent the residuals. Algorithm 1 shows how non-linear iterative partial least squares (NIPALS) solves these equations. NIPALS is able to retain discriminative information by exchanging the scores  $u_i$  and  $t_i$  while factorizing  $X$  and  $Y$  [7]. We execute the algorithm separately for each column of  $Y$  to avoid interference between the attributes on the projected space.

We also provide a fine-grained analysis of each layer of the network to identify filters and neurons that encode relevant information for attribute prediction. To this end, we employ VIP [18] to measure how much each feature, or neural output, of original high-dimensional space contributes to the discriminative low-dimensional projection.

---

#### Algorithm 1: NIPALS

---

**input :**  $X \in \mathbb{R}^{n \times m}$ ,  $y \in \mathbb{R}^{n \times 1}$ ,  $k \in \mathbb{I}$   
**output:**  $W^* \in \mathbb{R}^{m \times k}$

```

1  $E = X$ ;
2  $f = y$ ;
3 for  $i \leftarrow 1$  to  $k$  do
4   randomly initialize  $u_i \in \mathbb{R}^{n \times 1}$ ;
5   repeat
6      $w_i = \frac{E^T u_i}{\|E^T u_i\|}$ ;
7      $t_i = E w_i$ ;
8      $q_i = \frac{f^T t_i}{\|f^T t_i\|}$ ;
9      $u_i = f q_i$ ;
10  until  $w_i$  reaches convergence;
11   $p_i = E^T t_i$ ;
12   $E = E - t_i p_i^T$ ;
13   $f = f - t_i q_i^T$ ;
14  $W^* = W(PW)^{-1}$ ;
```

---

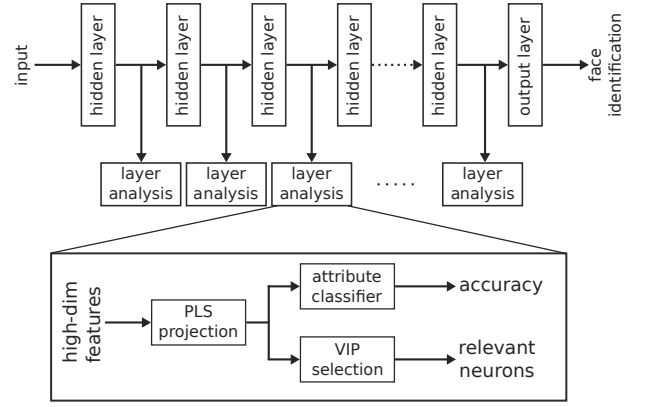


Fig. 2. For each attribute, we learn a discriminative low-dimensional projection using the high-dimensional output of the deep network layer. The low-dimensional projection is used to measure how well the layer encodes an attribute, and to identify the most relevant neurons. The process is repeated for each convolutional layer of the DCNN.

The VIP score of the  $j$ th neuron is determined by

$$\text{VIP}(j) = \sqrt{m \sum_{i=1}^k \frac{SS_i \frac{W_{ij}}{\|W_i\|^2}}{\sum SS_i}}, \quad (3)$$

where  $m$  and  $k$  are the original and the projection dimensionalities respectively, and  $SS_i$  is the sum of squares explained by the  $i$ th component, which can be alternatively expressed as  $q_i^2 t_i^T t_i$ .

Fig. 2 summarizes our approach. For each layer in the network, we learn a low-dimensional projection using PLS, which is then used to train a simple classifier for each attribute. This produces a performance curve for each attribute over the network depth, showing how and where the network learns each attribute. We also apply VIP technique over the PLS projection to determine the relevant neurons of each layer. Furthermore, we also propose to obtain the importance of each filter by averaging the VIP score of its neurons. The proportion of relevant neurons/filters at each layer reveals whether the attributes information is concentrated in a few units or entangled throughout the entire layer. Finally, we also measure the performance of the classifier when only the relevant neurons/filters are available as input so that we can quantify the efficiency of the VIP selection technique.

#### IV. EXPERIMENTAL RESULTS

Our face recognition networks are trained on the VGGFace2 [2] dataset, using the LFW [10] dataset as validation. We followed the standard training protocol [2], using uniform sampling of the identities, randomly cropping a  $224 \times 224$  region from the resized image of which the shorter side is 256 pixels, and transforming the image to grayscale with a 20% chance. We adopt ResNet50 [9] as our architecture because it provides a strong performance on recognition tasks while still being fairly linear, which allows us to represent the network performance as a line chart.

We use 40 binary attributes from the CelebA [16] dataset to help us understand the recognition network. Unless stated



Fig. 3. Attribute accuracy over the network depth. The blue curve measures the accuracy when the entire layer output is used to predict the attribute. The green and orange curves measure the accuracy when only the best eight filters or neurons, respectively, are used for prediction.

otherwise, all experiments were performed on the training and validation splits of this dataset. Even though PLS is more efficient than other classic learning methods [24], it still cannot load the entire training set on memory. For each attribute, we sample 2,048 faces for training, and 6,144 for validation from the original training and validation splits combined. For all attributes, half the samples are positive labels, and thus, there are no biases in our initial analysis.

We trained a PLS model to learn a projection of 8 components for each attribute and layer output. Each projection was used to train a QDA classifier, which we then evaluate on a validation set. The dark blue curve in Fig. 3 shows the achieved accuracy for each attribute as a function of the

DCNN feature depth averaged over six experiments. Each experiment is a different random optimization of the ResNet50 architecture, but the training and validation splits for the face attributes are maintained throughout the experiments.

The general behavior of the curves is either an early plateau or a modest slope after the first few layers. This indicates that these shallow features are discriminative enough, or at least competitive against deeper features, for most of the evaluated attributes. Previous works suggest that shallow features are only capable of capturing low level information such as textures and edges [17, 34]. Human operators may visualize these features and assign no meaning to them, while their high accuracy indicates that they already encode

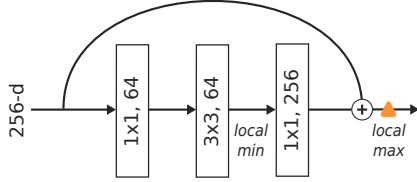
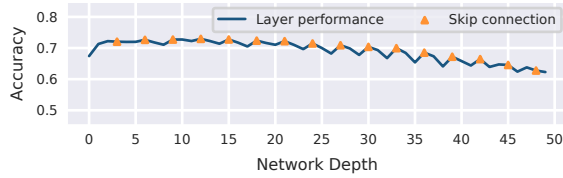


Fig. 4. Top: entire layer performance of the attribute Narrow Eyes. Bottom: residual block from the ResNet50 architecture. The performance curve exhibits a sawtooth pattern due to skip connections and bottlenecks present in the residual block.

relevant semantic information. A contrasting hypothesis is that these features are so high-dimensional that they are discriminative of any simple attribute, i.e., a bag of any set of shallow features would also be discriminative of these attributes. However, it remains unclear why some semantically equivalent attributes have such vastly different performances, e.g., gray hair is more accurately predicted than brown hair.

Interestingly, some soft-biometric attributes such as *Wearing Hat* and *Eyeglasses* have exceptional accuracy. This means that the network encodes such attributes, and that they are relevant for the face recognition task. In a surveillance scenario, these attributes could compromise the performance of the recognition system since, in this setting, the system cannot rely on the individual wearing his usual attire. However, in the context of the VGGFace2 dataset optimization, it is intuitive that each identity has some accessories of preference, and thus, the DCNN uses this information as a cue for recognition.

Another interesting aspect is observed in the last row of Fig. 3. The performance of these attributes decreases as the network gets deeper. These attributes encode intra-class variations of an identity, and thus, are not discriminative for recognition. For instance, the pale skin attribute indicates a variation of increased brightness in a person with fair skin tone. Thus, the accuracy drop indicates that the deeper representations in the network are more robust to variations in brightness, blur or mouth pose.

The curves of the last row also exhibit a distinct sawtooth pattern. In fact, all other curves display, albeit more subtly, a similar pattern. Fig. 4 shows a more detailed visualization of the Narrow Eyes accuracy, which reveals that the sawtooth aspect is closely related to the ResNet50 design. This architecture is constructed with the concatenation of residual blocks, which contain three convolutional layers each. The first two layers of the block create a compact projection of the previous block, reducing the number of

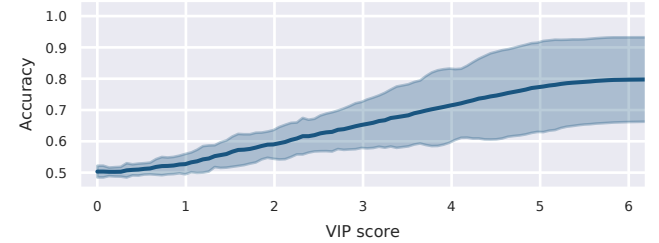
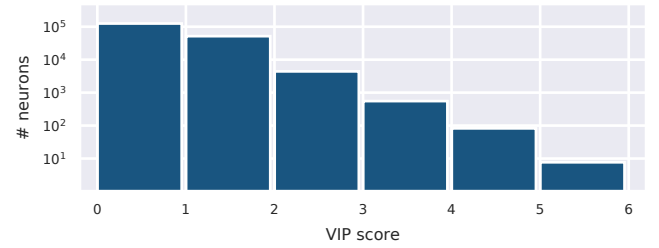


Fig. 5. Top: average distribution of the neural VIP score over all layers of the DCNN (please note the log-scale in the y-axis). Bottom: average accuracy using a single neuron as a feature, the shaded area represents two standard deviations. Both analysis were performed for the Male attribute.

filters of the representation, which is then restored at the third layer to be combined with the previous block through a skip-connection. Generally, the local maxima coincide with the skip-connections while the minima, with the two intermediary residual outputs. It seems that the sharp decreases indicate that some of the attribute information is discarded, possibly because it is not relevant for the recognition output.

We also analyze the performance of the neurons individually to understand how the information is distributed inside the layers. Fig. 5 shows the neural VIP score distribution and its average accuracy for the Male attribute. We record the VIP score of all neurons for each layer and report the average distribution over all layers (notice the log-scale). It is clear that high-scoring neurons are very scarce, suggesting that the information for each attribute is concentrated in only a few neurons. We then measure, for each layer, the classifier accuracy when only a single neuron is available as input, using 50 randomly selected neurons per layer, sampled uniformly with respect to their VIP score. The average performance shows, as expected, that the VIP score is a good indicator of which neurons encodes the relevant information.

Since the attribute information is concentrated in only a few neurons, our training process can be simplified to use the relevant neurons directly as input, without the need of projecting the output into a low-dimensional space. The orange curve in Fig. 3 shows the performance of the QDA classifier using the eight highest scoring neurons of each layer. For mid-level representations, the curves behave as expected, the classifier with eight neurons as input has a comparable accuracy to the one with the entire layer as input. However, for most attributes, there is a large performance gap in the first and last layers of the network. We believe that



	Male	Smiling	Eyeglasses	W. Hat	W. Lipstick	Wavy Hair	H. Cheekbones	Pointy Nose	Big Nose	Blurry	Brown Hair	Oval Face	Narrow Eyes	W. Necklace	Average
MOON [22]	-	-	-	-	-	-	-	-	-	-	-	-	-	-	90.9
AttCNN [8]	-	-	-	-	-	-	-	-	-	-	-	-	-	-	91.0
LNets + ANets [16]	98.0	92.0	99.0	99.0	93.0	80.0	87.0	72.0	78.0	84.0	80.0	66.0	81.0	71.0	87.0
Multitask	98.2	91.3	99.5	98.9	93.7	82.3	86.2	76.6	83.9	95.2	86.2	73.7	85.6	86.2	90.2
Best Layer	97.7	90.4	98.3	97.5	92.1	80.2	83.6	65.3	72.6	83.4	74.0	60.4	71.3	62.7	83.1
Best Filter	96.4	87.9	96.7	95.1	89.9	77.3	81.0	62.6	69.6	76.8	67.3	59.4	72.4	54.8	79.5
Best Neuron	96.2	83.4	96.1	96.3	89.6	70.5	78.8	65.3	68.7	69.8	64.2	60.3	75.2	54.7	77.4

TABLE I  
ACCURACY ON THE CELEBA TEST SET.



Fig. 6. Each column contains an average image for the highest (top) and the lowest (bottom) activation of a neuron. These are most discriminative neurons of the 34th layer, under the VIP criterion, for the Eyeglasses attribute.

the small receptive fields are the main reason of the poor performance in the first layers, as the neurons would have to make decisions based only on a partial input. For the last layers, it is possible that the neurons begin to be specialized for identification, and thus, the attribute information is spread out among many identities and neurons. The green curve in Fig. 3 shows the achieved accuracy when entire channels are selected, instead of neurons. We select eight channels from each layer and then project these channels into eight components with PLS. This time, the gaps in the initial layers are reduced, supporting our hypothesis that the shallow neurons lack the receptive field.

While one of our main goals was to avoid the subjectivity of visualizations, we provide a very simplistic representation of the neurons in the network to show a flaw that is present in many other techniques. First, we measure the activation of the top-8 neurons of an attribute, using all images in the test split of the CelebA dataset. Then, for each neuron, we create an average of the 100 images that produce the highest activations, and another average image for those with the lowest. Fig. 6 shows the obtained images for the top-8 neurons encoding the Eyeglasses attribute. We can notice that the attribute does not necessarily produce a high activation in the discriminative neuron, thus, maximization of hidden neurons does not necessarily produce good or even correct representations of what is really encoded.

Finally, we make a quantitative comparison between deep recognition features with state-of-the-art approaches for attribute prediction on the CelebA test set. Our goal here is to show that, for some of the attributes, the features of a recognition DCNN, which were not supervised for attribute recognition, are competitive against fully supervised deep

learning methods. We provide an additional baseline by finetuning each of our six models for attribute prediction, by simply replacing the identification output layer for an attribute prediction multitask layer. Table I shows the obtained performance for some attributes, as well as the average of all attributes. The best layer, filter and neuron were chosen based on their performance on the validation set. To reduce the number of candidates, the best filters and neurons were chosen based on a list of top-8 highest VIP scores for each layer of the model. For conciseness, we only report a few attributes, which highlight the best and worst attributes of our analysis, respectively on the left and right halves of the table. The reported average is calculated over all 40 attributes.

The average results achieved in Table I show that, for each attribute, a single neuron is less than 6 p.p. worse than an entire high-dimensional layer. Selecting the best filter diminishes this gap to less than 4 p.p., indicating that the attributes are captured by specific units in the network. The small gap can be explained by lack of robustness of a single filter or neuron, which may not be able to capture all variations of the attribute. The left half of Table I shows attributes in which the deep recognition features are less than 3 p.p. worse than a fully supervised multitask network.

## V. CONCLUSIONS AND FUTURE WORKS

While very effective, deeply learned representations are difficult to understand. Previous attempts to understand these representations were mainly based on subjective visualizations, which could lead to inaccurate conclusions. Through extensive experiments, we were able to quantitatively show that many face attributes are encoded inside a deep face recognition network. When compared to deep techniques that were fully supervised for attribute recognition, features from a face identification DCNN remain competitive, demonstrating that they are able to learn these concepts implicitly. Using our proposed method, we were able to evaluate high-dimensional layers of a deep network and identify the key feature points where each attribute information is encoded. Our analysis also revealed that these semantic concepts are highly concentrated on a few neurons, instead of being entangled in the entire layer. Furthermore, we observed that the neural information is not necessarily encoded with

maximal activations, which was an assumption made by many of the previous visualization techniques.

We also observed that a few similar attributes displayed vastly different performances, perhaps due to dataset biases or failures cases of deep representations, which we intend to further investigate in future works. Our analysis was focused on the ResNet50 architecture, revealing some interesting properties of the residual blocks. We believe that applying our proposed framework to different networks, could also expose new interesting properties and behaviors which may aid other researches to develop better architectures.

#### ACKNOWLEDGMENTS

The authors would like to thank the National Council for Scientific and Technological Development – CNPq (Grants 438629/2018-3 and 309953/2019-7), the Minas Gerais Research Foundation – FAPEMIG (Grants APQ-00567-14 and PPM-00540-17) and the Coordination for the Improvement of Higher Education Personnel – CAPES (DeepEyes Project and Finance Code 001).

#### REFERENCES

- [1] H. Abdi. Partial least squares regression and projection on latent structure regression (pls regression). *Wiley interdisciplinary reviews: computational statistics*, 2(1):97–106, 2010.
- [2] Q. Cao, L. Shen, W. Xie, O. M. Parkhi, and A. Zisserman. Vggface2: A dataset for recognising faces across pose and age. In *2018 13th IEEE International Conference on Automatic Face & Gesture Recognition (FG 2018)*, pages 67–74. IEEE, 2018.
- [3] J. Deng, J. Guo, N. Xue, and S. Zafeiriou. Arcface: Additive angular margin loss for deep face recognition. In *Proceedings of the IEEE Conference on Computer Vision and Pattern Recognition*, pages 4690–4699, 2019.
- [4] J. Deng, Y. Zhou, and S. Zafeiriou. Marginal loss for deep face recognition. In *Proceedings of the IEEE Conference on Computer Vision and Pattern Recognition Workshops*, pages 60–68, 2017.
- [5] A. Dosovitskiy and T. Brox. Inverting visual representations with convolutional networks. In *Proceedings of the IEEE Conference on Computer Vision and Pattern Recognition*, pages 4829–4837, 2016.
- [6] C. Ferrari, S. Berretti, and A. Del Bimbo. Discovering identity specific activation patterns in deep descriptors for template based face recognition. In *2019 14th IEEE International Conference on Automatic Face & Gesture Recognition (FG 2019)*, pages 1–5. IEEE, 2019.
- [7] P. Geladi and B. R. Kowalski. Partial least-squares regression: a tutorial. *Analytica chimica acta*, 185:1–17, 1986.
- [8] E. M. Hand, C. Castillo, and R. Chellappa. Doing the best we can with what we have: Multi-label balancing with selective learning for attribute prediction. In *Thirty-Second AAAI Conference on Artificial Intelligence*, 2018.
- [9] K. He, X. Zhang, S. Ren, and J. Sun. Deep residual learning for image recognition. In *Proceedings of the IEEE conference on computer vision and pattern recognition*, pages 770–778, 2016.
- [10] G. B. Huang, M. Mattar, T. Berg, and E. Learned-Miller. Labeled faces in the wild: A database for studying face recognition in unconstrained environments. 2008.
- [11] A. Jordao, R. Kloss, and W. R. Schwartz. Latent hypernet: Exploring the layers of convolutional neural networks. In *2018 International Joint Conference on Neural Networks (IJCNN)*, pages 1–7. IEEE, 2018.
- [12] A. Jordao, F. Yamada, and W. R. Schwartz. Pruning deep neural networks using partial least squares. *arXiv preprint arXiv:1810.07610*, 2018.
- [13] I. Kemelmacher-Shlizerman, S. M. Seitz, D. Miller, and E. Brossard. The megaface benchmark: 1 million faces for recognition at scale. In *Proceedings of the IEEE Conference on Computer Vision and Pattern Recognition*, pages 4873–4882, 2016.
- [14] T. Kong, A. Yao, Y. Chen, and F. Sun. Hypernet: Towards accurate region proposal generation and joint object detection. In *Proceedings of the IEEE conference on computer vision and pattern recognition*, pages 845–853, 2016.
- [15] A. Krizhevsky, I. Sutskever, and G. E. Hinton. Imagenet classification with deep convolutional neural networks. In *Advances in neural information processing systems*, pages 1097–1105, 2012.
- [16] Z. Liu, P. Luo, X. Wang, and X. Tang. Deep learning face attributes in the wild. In *Proceedings of the IEEE international conference on computer vision*, pages 3730–3738, 2015.
- [17] A. Mahendran and A. Vedaldi. Visualizing deep convolutional neural networks using natural pre-images. *International Journal of Computer Vision*, 120(3):233–255, 2016.
- [18] T. Mehmood, K. H. Liland, L. Snipen, and S. Sæbø. A review of variable selection methods in partial least squares regression. *Chemometrics and Intelligent Laboratory Systems*, 118:62–69, 2012.
- [19] A. Nguyen, J. Yosinski, and J. Clune. Multifaceted feature visualization: Uncovering the different types of features learned by each neuron in deep neural networks. *arXiv preprint arXiv:1602.03616*, 2016.
- [20] R. Ranjan, C. D. Castillo, and R. Chellappa. L2-constrained softmax loss for discriminative face verification. *arXiv preprint arXiv:1703.09507*, 2017.
- [21] R. Ranjan, S. Sankaranarayanan, C. D. Castillo, and R. Chellappa. An all-in-one convolutional neural network for face analysis. In *2017 12th IEEE International Conference on Automatic Face & Gesture Recognition (FG 2017)*, pages 17–24. IEEE, 2017.
- [22] E. M. Rudd, M. Günther, and T. E. Boult. Moon: A mixed objective optimization network for the recognition of facial attributes. In *European Conference on Computer Vision*, pages 19–35. Springer, 2016.
- [23] F. Schroff, D. Kalenichenko, and J. Philbin. Facenet: A unified embedding for face recognition and clustering. In *Proceedings of the IEEE conference on computer vision and pattern recognition*, pages 815–823, 2015.
- [24] W. R. Schwartz, A. Kembhavi, D. Harwood, and L. S. Davis. Human detection using partial least squares analysis. In *2009 IEEE 12th International Conference on Computer Vision (ICCV)*, pages 24–31. IEEE, 2009.
- [25] R. R. Selvaraju, M. Cogswell, A. Das, R. Vedantam, D. Parikh, and D. Batra. Grad-cam: Visual explanations from deep networks via gradient-based localization. In *Proceedings of the IEEE International Conference on Computer Vision*, pages 618–626, 2017.
- [26] M. S. Shafiee, M. J. Shafiee, and A. Wong. Efficient inference on deep neural networks by dynamic representations and decision gates. *arXiv preprint arXiv:1811.01476*, 2018.
- [27] K. Simonyan, A. Vedaldi, and A. Zisserman. Deep inside convolutional networks: Visualising image classification models and saliency maps. *arXiv preprint arXiv:1312.6034*, 2013.
- [28] Y. Sun, Y. Chen, X. Wang, and X. Tang. Deep learning face representation by joint identification-verification. In *Advances in neural information processing systems*, pages 1988–1996, 2014.
- [29] Y. Sun, X. Wang, and X. Tang. Deeply learned face representations are sparse, selective, and robust. In *Proceedings of the IEEE conference on computer vision and pattern recognition*, pages 2892–2900, 2015.
- [30] C. Szegedy, W. Zaremba, I. Sutskever, J. Bruna, D. Erhan, I. Goodfellow, and R. Fergus. Intriguing properties of neural networks. *arXiv preprint arXiv:1312.6199*, 2013.
- [31] J. Yosinski, J. Clune, A. Nguyen, T. Fuchs, and H. Lipson. Understanding neural networks through deep visualization. *arXiv preprint arXiv:1506.06579*, 2015.
- [32] M. D. Zeiler and R. Fergus. Visualizing and understanding convolutional networks. In *European conference on computer vision*, pages 818–833. Springer, 2014.
- [33] K. Zhao, J. Xu, and M.-M. Cheng. Regularface: Deep face recognition via exclusive regularization. In *Proceedings of the IEEE Conference on Computer Vision and Pattern Recognition*, pages 1136–1144, 2019.
- [34] Y. Zhong and W. Deng. Exploring features and attributes in deep face recognition using visualization techniques. In *2019 14th IEEE International Conference on Automatic Face & Gesture Recognition (FG 2019)*, pages 1–8. IEEE, 2019.
- [35] B. Zhou, A. Khosla, A. Lapedriza, A. Oliva, and A. Torralba. Object detectors emerge in deep scene cnns. *arXiv preprint arXiv:1412.6856*, 2014.
- [36] B. Zhou, A. Khosla, A. Lapedriza, A. Oliva, and A. Torralba. Learning deep features for discriminative localization. In *Proceedings of the IEEE conference on computer vision and pattern recognition*, pages 2921–2929, 2016.